# THE INFLUENCE OF THE STRAIN RATE ON THE VALUE OF FRICTION COEFFICIENT

**PETR SVOBODA[1], MIROSLAV JOPEK[1]**

[1]Brno University of Technology, Faculty of Mechanical Engineering, Institute of Manufacturing Technology, Department of Metal Forming and Plastics, Brno, Czech Republic

**DOI: 10.17973/MMSJ.2024_12_2024031**

**e-mail: 209148@vutbr.cz**

The Male and Cockroft ring compression test stands as one of the methods utilized to determine the coefficient of friction in forming processes. This approach eliminates the need for force measurement. This study presents the outcomes of the Male and Cockroft ring compression test conducted on Hardox 450 material at varying strain rates, conducted without lubricant. The experiments were carried out using a ZD-40 hydraulic press, CFA-80 pneumatic die hammer and split Hopkinson pressure bar test at the Faculty of Mechanical Engineering of Brno University of Technology. The test results were documented on a calibration diagram, revealing a significant influence of strain rate on the coefficient of friction. Specifically, the findings indicate that as the strain rate increases, the coefficient of friction decreases.

**KEYWORDS**

strain rate, friction, ring compression test, Hardox 450 steel, split Hopkinson pressure bar test

## 1 INTRODUCTION

In the bulk forming industry today, the primary focus is on advancing processing technologies to boost efficiency and productivity. Modern automatic sequential machines, which can produce between 300 and 600 parts per minute, are especially favored in mass production [Hammer 2016]. During manufacturing, strain rates can reach up to $10^4$ $s^{-1}$. Recently, high-speed forming has been employed to produce complex components at room temperature. Plastic forming techniques, such as high-speed forming, impact hydroforming, and electromagnetic forming are gaining popularity [Chen 2021, Kinsey 2019].

Friction occurring at the interface between the semi-finished product and the forming tool plays a critical role in both the quality of the final produced part and the efficiency of the forming process. Its impact extends to various aspects such as flow stress, forming force, required specific work, material flow behavior, surface quality, temperature development, and tool wear [Joun 2009]. Therefore, accurately determining the friction coefficient is essential for optimizing the manufacturing process.

In the realm of bulk forming techniques like forging, extrusion, ramming etc., friction coefficient maps, originally introduced by Kunogi through the ring compression test, have been employed [Kunogi 1957]. This testing method was subsequently refined by Male and Cockroft [Male 1965]. These graphical representations offer a straightforward approach to ascertain the friction coefficient between the workpiece and the forming tool's contact surface.

Initially, it was believed that the calibration diagrams were universally applicable to material groups (such as steel, cast iron, titanium alloy etc.) and were solely dependent on the dimensions of the ring. However, subsequent research revealed the necessity to develop separate calibration diagrams for each material with specific chemical composition, thus discrediting the assumption of universality across material groups [Camacho 2013]. Upon further investigation into the frictional process, it was uncovered that the friction coefficient's magnitude is contingent upon the temperature of both the material being worked and the forming tools [Wang 2023].

Recently, there has been a growing interest in assessing the tribological properties of materials over the entire spectrum of strain rates [Svoboda 2024a]. The fabrication of components by forming usually involves higher strain rates because the quasi-static rates at which most material testing takes place are rarely encountered in forming processes, i.e. hydroforming or superplastic forming processes.

## 2 RING COMPRESSION TEST

Among the various techniques employed to ascertain the coefficient of friction between the blank surface and the forming tool, the ring compression test stands out as the prevailing standard. This method operates on the principle of observing alterations in the inner and outer diameter of the ring upon compression, leading to a phenomenon known as 'bulging'. If the inner diameter expands during compression, indicating low friction (Fig. 1). Conversely, if the inner diameter contracts during compression, it suggests high friction (Fig. 2).

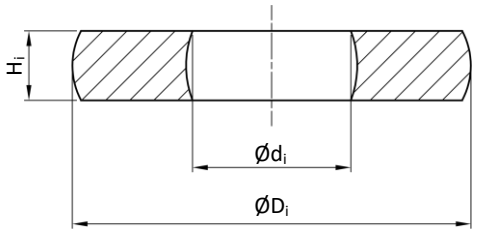


**Figure 1.** Low friction (good lubrication)

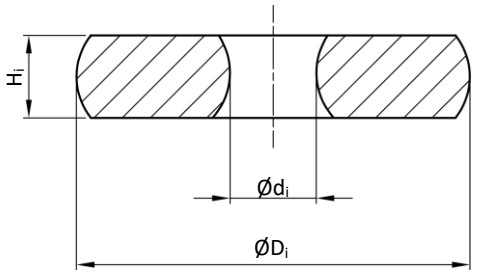


**Figure 2.** High friction (poor lubrication)

Taking into account these dependencies, calibration curves (sometimes also called as friction maps) were formulated to accurately determine the coefficient of friction. Male & Cockroft devised this curve specifically for samples featuring a 6:3:2 geometry ratio, where 6 represents the outer diameter D, 3 denotes the inner diameter d, and 2 signifies the height H (Fig. 3). Subsequently, this ratio was adopted as the standard [Partovi 2019].

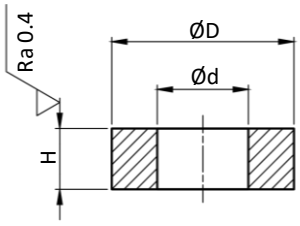


**Figure 3.** Sample before loading

The following equations are used to evaluate the change in ring height and inner diameter:

$$\varepsilon_d = \frac{d - d_i}{d} \cdot 100\ [\%] \quad (1)$$

$$\varepsilon_H = \frac{H - H_i}{H} \cdot 100\ [\%] \quad (2)$$

where:

$\varepsilon_d$ ..... deformation of the inner diameter of the ring [%],

$d$ ..... initial inner diameter of the ring [mm],

$d_i$ ..... final inner diameter of the ring [mm],

$\varepsilon_H$ ..... deformation of height of the ring [%],

$H$ ..... initial height of the ring [mm],

$H_i$ ..... final height of the ring [mm].

The simplicity of applying calibration diagrams lies in establishing the relationship between the alteration in the inner diameter of the ring and the change in its height. These curves are subsequently graphed for each friction coefficient $f$ or friction factor $m$ (Fig. 4). An exceptional advantage of this method is the absence of necessity to measure forces during testing, coupled with the sufficiently substantial deformations that can be conveniently measured using conventional gauges. Moreover, this test serves as a valuable tool for assessing the effectiveness of different lubricants in forming processes.

For conversion between friction coefficient and friction factor mentioned above, following equation based on plasticity condition according to Hency, Mises, and Huber (HMH) is used:

$$f = \frac{m}{\sqrt{3}}\ [1] \quad (3)$$

where:

$f$ ..... friction coefficient [1],

$m$ ..... friction factor [1].

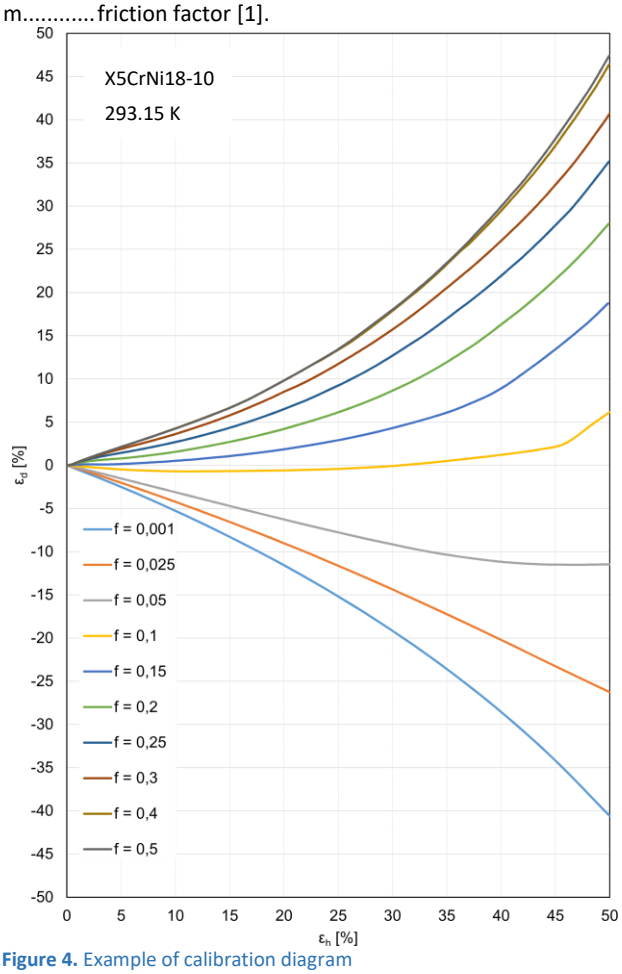


**Figure 4.** Example of calibration diagram

## 3 MATERIALS AND METHODS

### 3.1 Material and Geometry of Specimens

Today, an increasing number of components traditionally made from structural steel are being replaced with high-strength steel alternatives. This shift is especially evident in industries like mining, forestry, and automotive manufacturing. High-strength steel components offer superior mechanical properties, allowing for the production of smaller, lighter parts. This reduction in component weight leads to decreased transport costs and lower $CO_2$ emissions, aligning with the growing focus on sustainability.

For these purposes the high-strength Hardox 450 steel (for chemical composition see Tab. 1) was chosen as the material of the samples. Rings with nominal dimensions of 8:4:2.667 were used for testing. Contact surfaces between ring and tool were grinded on plane grinder to roughness Ra = 0.4 µm. For ring compression tests no lubricant was used.

| Element | C | Si | Mn | P | S |
|---|---|---|---|---|---|
| wt. % | 0.18 | 0.27 | 0.96 | 0.007 | 0.003 |
| Element | Cr | Ni | Mo | B | Fe |
| wt. % | 0.11 | 0.08 | 0.027 | 0.001 | rest |

**Table 1.** Chemical composition of Hardox 450 steel

### 3.2 Experimental methods

The quasi-static compression tests at low strain rates were performed on a ZD-40 hydraulic press equipped with load cell up to 400 kN (Fig. 5). Crosshead speeds of 0.5 mm·min$^{-1}$ and 200 mm·min$^{-1}$ were used. Tool movement speeds were set and controlled by hydraulic gear pump. During compression process on hydraulic presses, a constant speed of tool movement is achieved. This makes it possible to use the following equation to calculate the deformation rate:

$$\dot{\varphi} = \frac{v \cdot \ln\left(\frac{H}{H_i}\right)}{H - H_i}\ [s^{-1}] \quad (4)$$

where:

$\dot{\varphi}$ ..... strain rate [s$^{-1}$],

$v$ ..... tool movement speed [mm·s$^{-1}$].

**Figure 5.** ZD-40 hydraulic press

Tests during medium strain rates were performed CFA-80 pneumatic die hammer with 80 kJ impact work (Fig. 6). Tool

movement speed of 0.8 m·s$^{-1}$ was used. Tool movement speed was measured by high-speed camera. Because tool movement speed of die hammer is not constant equation (4) cannot be used for calculation strain rate. For these reasons mean strain rate is calculated from strain rate values through time, Fig. 7. Equation used for calculating mean strain rate is:

$$\dot{\varphi}_{mean} = \frac{\sum(\dot{\varphi}_i + \dot{\varphi}_{i-1}) \cdot (\tau_{i+1} - \tau_i)}{2 \cdot (\tau_{end} - \tau_0)} \; [s^{-1}] \qquad (5)$$

where:

$\dot{\varphi}_{mean}$ .... mean strain rate [s$^{-1}$],

$\tau$ ..... time [s],

$\tau_0$ ..... initial time [s],

$\tau_{end}$ ..... end time [s].


**Figure 6.** CFA-80 pneumatic die hammer

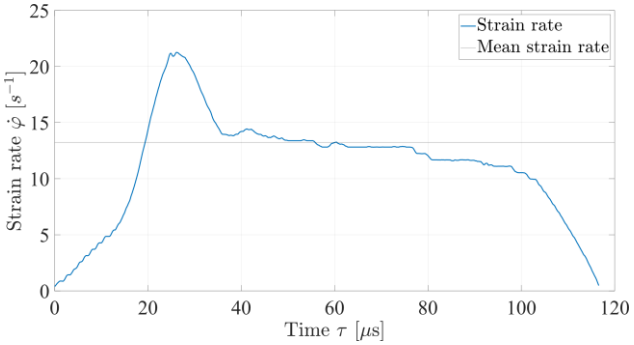


**Figure 7.** Strain rate-time dependance

Dynamic compression test at high strain rates were performed on split Hopkinson pressure bar test (SHPBT), Fig. 8. This is one of devices that are commonly used for determination dynamic behaviour of materials [Jopek 2021, Svoboda 2024b, Harant 2024]. Tool movement speeds of 25 m·s$^{-1}$ and 40 m·s$^{-1}$ were used. Tool movement speeds were measured by laser speed measurement which is included in device. Equation (5) was used to determine the mean strain rate.

**Figure 8.** Split Hopkinson pressure bar test

The testing conditions for each device such as temperature, tool movement speed and strain rate are given in Tab. 2.

| Machine | ZD-40 | ZD-40 | CFA-80 |
|---|---|---|---|
| Temperature [K] | 291,15 | 291,15 | 291,15 |
| Tool movement speed [m·s$^{-1}$] | 8.333·10$^{-6}$ | 3.333·10$^{-3}$ | 0.8 |
| Strain rate [s$^{-1}$] | 4.461·10$^{-6}$ | 1.462 | 13.241 |
| Machine | SHPBT | | SHPBT |
| Temperature [K] | 291,15 | | 291,15 |
| Tool movement speed [m·s$^{-1}$] | 25 | | 40 |
| Strain rate [s$^{-1}$] | 9.861·10$^{2}$ | | 3.015·10$^{3}$ |

**Table 2.** Testing conditions

## 4 RESULTS AND DISCUSSION

For each strain rate were performed 5 tests. From these tests mean values were calculated and then entered into calibration diagram, Fig. 9. The friction coefficient values that were read from the graph in Fig. 9 are shown in the Tab. 3. For better comparison were values also recalculated to friction factor using equation (3).

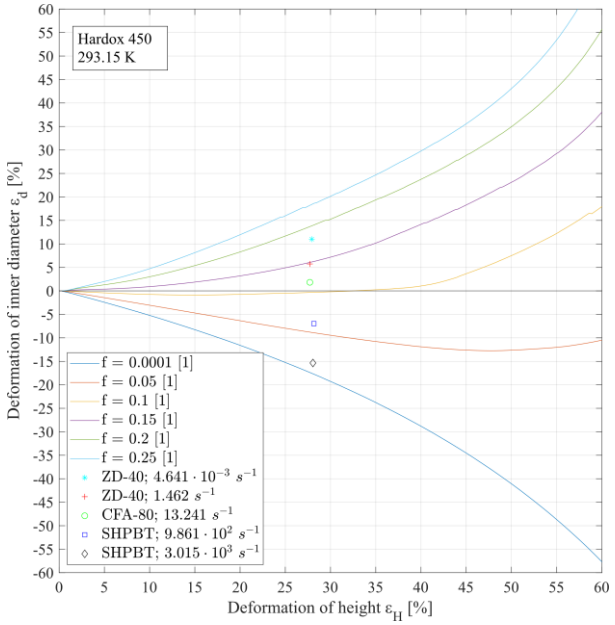


**Figure 9.** Hardox 450 – calibration diagram with measured values

| Friction coefficient f [1] | Friction factor m [1] | Strain rate $\dot{\varphi}$ [$s^{-1}$] |
|---|---|---|
| 0.181 | 0.314 | $4.461 \cdot 10^{-6}$ |
| 0.149 | 0.258 | 1.462 |
| 0.119 | 0.206 | 13.241 |
| 0.063 | 0.109 | $9.861 \cdot 10^{2}$ |
| 0.010 | 0.017 | $3.015 \cdot 10^{3}$ |

**Table 3.** Obtained values of friction at different strain rates

The findings from the Male and Cockroft ring compression test reveal a clear relationship between strain rate and the friction coefficient in Hardox 450 steel under various testing conditions. As shown in Fig. 9, although the height deformation of the ring remains constant, the deformation in the inner diameter varies (Fig. 10), resulting in different friction coefficient values across strain rates. This variation can be attributed to how the contact interface and frictional interactions change with strain rate. Specifically, the highest friction coefficient observed is 0.181 at a quasi-static strain rate of $4.461 \cdot 10^{-6}$ $s^{-1}$, whereas the lowest is 0.010 at a dynamic strain rate of $3.015 \cdot 10^{3}$ $s^{-1}$. This trend suggests that at higher strain rates, the friction coefficient decreases.


**Figure 10.** Specimens after ring compression test **(a)** strain rate $4.461 \cdot 10^{-6}$ $s^{-1}$; **(b)** strain rate 1.462 $s^{-1}$; **(c)** strain rate 13.241 $s^{-1}$; **(d)** strain rate $9.861 \cdot 10^{2}$ $s^{-1}$ and **(e)** strain rate $3.015 \cdot 10^{3}$ $s^{-1}$

As illustrated in Fig. 11, this inverse relationship between friction coefficient and strain rate highlights that under dynamic conditions, frictional forces at the interface are reduced. Lower friction at high strain rates can have practical implications, especially in forming operations where reducing friction could lead to lower required forming forces, extending tool life, and improving surface quality. The findings align with the conclusions of other studies, which show that dynamic conditions typically reduce the frictional resistance between tools and workpieces, enhancing material flow and reducing energy input requirements.

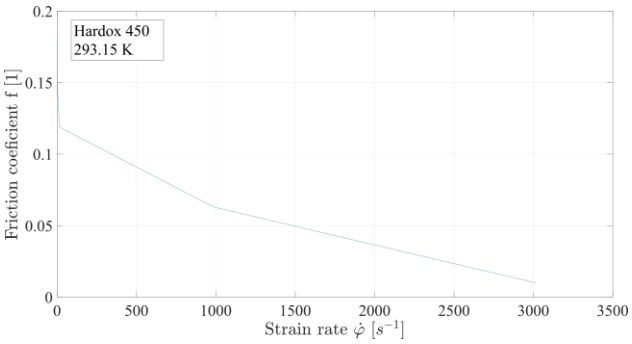


**Figure 11.** Friction coefficient-strain rate dependance

Overall, these results emphasize the importance of adjusting friction models to account for strain rate effects, as using friction coefficients derived only from quasi-static conditions may lead to overestimations of required forming forces in high-speed manufacturing processes. Consequently, this insight supports more accurate modeling and simulation, enabling optimized process parameters that balance material flow with minimal frictional resistance, thereby improving efficiency and durability in industrial applications.

## 5 CONCLUSIONS

This study demonstrates the significant effect of strain rate on the friction coefficient during the compression of Hardox 450 steel, using the Male and Cockroft ring compression test. The results show a clear trend in which the friction coefficient decreases as the strain rate increases, with values ranging from 0.181 at a quasi-static rate to 0.010 under dynamic conditions. This relationship indicates that as deformation speeds increase, the resistance due to friction at the interface decreases. These findings highlight the necessity of accounting for strain rate-dependent friction coefficients in high-speed bulk forming processes to improve the accuracy of predictive models.

In practical terms, incorporating dynamic friction values can lead to more efficient forming processes by reducing the force required and extending tool life, while also ensuring better material flow. By aligning the friction coefficient with the specific strain rate conditions of industrial applications, these results support the development of optimized manufacturing parameters that enhance both performance and durability in metal forming.


## ACKNOWLEDGMENTS

The article was recommended by the Scientific Committee from the international conference MANUFACTURING TECHNOLOGY PILSEN 2024.


## REFERENCES


**[Camacho 2013]** CAMACHO, A.M.; TORRALVO, A.I.; BERNAL, C. and SEVILLA, L., 2013. Investigations on Friction Factors in Metal Forming of Industrial Alloys. *Procedia Engineering.* Volume 63, Pages 564-572. Available from: https://doi.org/10.1016/j.proeng.2013.08.240.

**[Hammer 2016]** HAMMER, Jacob, 2016. Automatic defensive control of asynchronous sequential machines. *International Journal of Control.* Volume 89, Issue 1, Pages 193-209. ISSN 0020-7179. Available

from: https://doi.org/10.1080/00207179.2015.1064547.

[Chen 2021] CHEN, Da-Yong; XU, Yong; ZHANG, Shi-Hong; MA, Yan; EL-ATY, Ali Abd et al., 2021. a novel method to evaluate the high strain rate formability of sheet metals under impact hydroforming. *Journal of Materials Processing Technology.* Volume 287, Issue 116553. ISSN 0924-0136. Available from: https://doi.org/10.1016/j.jmatprotec.2019.116553.

[Kinsey 2019] KINSEY, Brad and KORKOLIS, Yannis, 2019. High-Speed Forming (Electromagnetic, Electrohydraulic, and Explosive Forming). In: *Modern Manufacturing Processes.* Pages 265-294. ISBN 978-1-11912-038-4. Available from: https://doi.org/10.1002/9781119120384.ch11.

[Harant 2024] HARANT, Martin; VERLEYSEN, Patricia; FOREJT, Milan and KOLOMY, Stepan, 2024. The Effects of Strain Rate and Anisotropy on the Formability and Mechanical Behaviour of Aluminium Alloy 2024-T3. *Metals.* Volume 14, Issue 1, Pages 98-110. Available from: https://doi.org/10.3390/met14010098.

[Jopek 2021] JOPEK, Miroslav; FOREJT, Milan and HARANT, Martin, 2021. MECHANICAL PROPERTIES OF ALUMINIUM ALLOYS AT HIGH STRAIN RATE. *MM Science Journal.* Volume 13, Issue 2, Pages 4505-4511. Available from: https://doi.org/10.17973/MMSJ.2021_6_2021050.

[Joun 2009] JOUN, M.S.; MOON, H.G.; CHOI, I.S.; LEE, M.C. a JUN, B.Y, 2009. Effects of friction laws on metal forming processes. *Tribology International.* Volume 42, Issue 2, Pages 311-319. ISSN 0301-679X.

[Kunogi 1957] KUNOGI, Mahito, 1957. A New Method of Cold Extrusion. *Transactions of the Japan Society of Mechanical Engineers.* Volume 23, Issue 134, Pages 742-749. Available from: https://doi.org/10.1299/kikai1938.23.742.

[Male 1965] MALE, A. and COCKROFT, M., 1965. A Method for the Determination of Coefficient of Friction of Metals under Condition of Bulk Plastic Deformation. *Journal of Institute of Metals.* Volume 93, Pages 38-46.

[Partovi 2021] PARTOVI, Amir; SHAHZAMANIAN, M. M. and WU, P. D., 2021. Numerical study of mechanical behaviour of tubular structures under dynamic compression. *Journal of Mechanical Science and Technology.* Volume 35, Issue 3, pages 1129-1142. ISSN 1976-3824. Available from: https://doi.org/10.1007/s12206-021-0226-8.

[Svoboda 2024a] SVOBODA, Petr and JOPEK, Miroslav, 2024. The effect of strain rate on the friction coefficient. *MANUFACTURING TECHNOLOGY.* Volume 24, Issue 2. Available from: https://doi.org/10.21062/mft.2024.027.

[Svoboda 2024b] SVOBODA, Petr; JOPEK, Miroslav; SVOBODA, Ondrej and HARANT, Martin, 2024. DETERMINATION OF DYNAMIC PROPERTIES OF 3D PRINTED G3SI1 STEEL. *MM Science Journal.* Volume 16, Issue 1, Pages 7230-7233. Available from: https://doi.org/10.17973/MMSJ.2024_03_2021183.

[Wang 2023] WANG, Wen and ZHOU, Xiang, 2023. Temperature-dependent friction coefficient on flat graphite plane. *Surface Science.* Volume 729, Pages 122-233. Available from: https://doi.org/10.1016/j.susc.2022.122233.

**CONTACTS:**

Ing. Petr Svoboda

Brno University of Technology, Faculty of Mechanical Engineering, Institute of Manufacturing Technology, Department of Metal Forming and Plastics

Technická 2896/2, Brno, 616 69, Czech Republic

e-mail: 209148@vutbr.cz

Ing. Miroslav Jopek, Ph.D.

Brno University of Technology, Faculty of Mechanical Engineering, Institute of Manufacturing Technology, Department of Metal Forming and Plastics

Technická 2896/2, Brno, 616 69, Czech Republic

e-mail: jopek@fme.vutbr.cz